Agricultural and Forest Meteorology 248 (2018) 130–144

Contents lists available at ScienceDirect

Agricultural and Forest Meteorology

journal homepage: www.elsevier.com/locate/agrformet

Influence of climate variability and length of rainy season on crop yields in semiarid Botswana

Jimmy Byakatonda[a,c,*], B.P. Parida[a], Piet K. Kenabatho[b], D.B. Moalafhi[b]

[a] Department of Civil Engineering, P/Bag 0061, University of Botswana, Gaborone, Botswana
[b] Department of Environmental Science, P/Bag 00704, University of Botswana, Gaborone, Botswana
[c] Department of Biosystems Engineering, Gulu University, P.O. Box 166, Gulu, Uganda

ARTICLE INFO

Keywords:
Aridity index
Artificial neural network
Correlation
ENSO
Southern oscillation index
Standardised precipitation evapotranspiration index

ABSTRACT

Climate variability and change is expected to affect agricultural productivity among other sectors. Studying the influence of this variability on crop production is one measure of generating climate change resilience strategies. In this study, the influence of climate variability on crop yield is investigated by determining the degree of association between climatic indices and crop yields of maize and sorghum using spearman's rank correlation. The climatic indices used in this study are aridity index (AI), standardised precipitation evapotranspiration index (SPEI) at timescales of 1, 3, 6 and 12 months and southern oscillation index (SOI) representing El Niño southern oscillation (ENSO) influence on local climate. Local rainfall characteristics are expressed through length of the rainy season (LRS). Results reveal that ENSO influence is the most dominant across Botswana accounting for 85% and 78% variations in maize and sorghum yields respectively. Whereas AI and SPEI accounts for 70% and 65% variations in maize and sorghum respectively, LRS accounts for only 50% and 62% respectively. To facilitate agricultural planning, crop yield projections have been made using artificial neural network (ANN) models. The ANN projections indicate a likelihood of maize and sorghum yields declining by 51% and 70% respectively in the next 5 years. The high association between ENSO and crop yields in Botswana could further facilitate yield projections. Information generated from this study is useful in agricultural planning and hence strengthens farmers' strategies in mitigating impacts of climate variability and change in semiarid areas.

1. Introduction

Increasing human population comes with an increase in demand for energy and food, leading to generation and eventual release of more greenhouse gases into the atmosphere to meet these demands (Some'e et al., 2013; Vörösmarty et al., 2000). Continued buildup of these greenhouse gases in the atmosphere has been closely associated with rising global temperature, reduced rainfall and increased climate variability in general exerting pressure on agricultural water resources and hence on crop yields (Hansen et al., 2010; Rockström et al., 2009). Attempts have been made globally to increase food production through technological and infrastructural improvements. Besides this, high variations are still reported mainly attributed to climate disasters that have ravaged the world in recent decades mainly in the form of frequent droughts (Alexandratos et al., 2012; Cabas et al., 2010; Li et al., 2009). Droughts have been identified as the single most important climatic hazard affecting agricultural production according to Helmer and Hilhorst (2006), Li et al. (2009) and Sivakumar (2011). In the advent of climate change and an increase in climate variability, drought frequency and severity are expected to worsen with far reaching impacts felt in semiarid and arid locations further exacerbating the already declining crop yields (Byakatonda et al., 2016; Khan et al., 2016; Modarres and da Silva, 2007; Omoyo et al., 2015). Semiarid locations could also propagate into arid and hyper arid climates as a result of climate change if no adaptation measures are put in place (Some'e et al., 2013; Zhang et al., 2009). Further still, in developing countries where absorption of improved technologies is still low and with existence of poor infrastructure, impacts of climate variability and change are expected to be more severe (Hatfield et al., 2011; Sivakumar, 2011). Climate variability and change have been found to shift the onset and cessation of rain hence affecting the length of the rainy season (Amekudzi et al., 2015; Mugalavai et al., 2008). This revelation brings uncertainty to regular and timely water supply necessary for replenishing soil moisture putting livelihoods depending on rainfed agriculture more at risk. Various attempts have been made to evaluate the effect of climate variability and change on crop yields. At a global scale, Li et al. (2009), investigated the risk of climate change on crop yields using parametric methods to establish correlations between

* Corresponding author at: Department of Civil Engineering, P/Bag 0061, University of Botswana, Gaborone, Botswana.
E-mail addresses: byakatondaj@hotmail.com, jbyaks@gmail.com (J. Byakatonda).

http://dx.doi.org/10.1016/j.agrformet.2017.09.016
Received 2 March 2017; Received in revised form 18 September 2017; Accepted 21 September 2017

Table 1
Agricultural regions with respective synoptic stations and locations where yields were collected.

Agricultural Region	Synoptic Stations	Locations for crop data
Southern	SSKA, Jwaneng and Tsabong	Barolong, Ngwaketse South, Ngwaketse North, Tlokweng, Kweneng South, Kweneng North and Kgatleng
Central	Mahalapye	Mahalapye, Palapye and Serowe
Eastern	Francistown, Letlhakane and Selibe-Phikwe	Bobonong, Letlhakane, Selebi-Phikwe, Tati, Tutume, Mmadinare
Northern	Shakawe, Maun and Kasane	Ngamiland West, Ngamiland East and Chobe
Western	Ghanzi, Tshane and Tsabong	Ghanzi, Hukuntsi and Tsabong

climate variables and crop yields. They also simulated future drought risks using outputs from 20 General Circulations Models (GCMs). Their findings revealed that, the African continent is more vulnerable to climate variability and change than any other region of the world. Studies in other semiarid areas of Asia such as Iran by Bannayan et al. (2011, 2010) revealed that variability in temperature and climatic indices substantially affected barley and wheat yields. They also used parametric techniques to quantify relationships between climatic variables and crop yields. In semiarid areas of Kenya, Omoyo et al. (2015) investigated the relationship between climate variability and yields of maize using regression analysis. Their findings revealed that maize yields were declining with decreasing trends in rainfall amidst warming trends. Rowhani et al. (2011) while studying impact of climate variability on yields of maize and sorghum in Tanzania used linear mixed models. Their findings indicated that by the middle of the century, a temperature rise of up to 2 °C may lead to reduction in yields of around 10% for these crops under investigation. Earlier studies as explained above have used parametric correlation methods hence assuming a normal distribution in crop yields and climatic variables. Due to climate dynamics and uncertainties under changing environment, with influences from external predictors such as El Niño southern oscillation (ENSO), a normal distribution may not necessarily hold. Hence this study proposes the use of non parametric rank based correlation method to study the degree of association between climatic indices and crop yields. The influences of ENSO on southern Africa's climate has been well articulated in studies by Nicholson et al. (2001), Usman and Reason (2004) and Edossa et al. (2014). Botswana located in the subtropics with more than 80% of its population engaged in rainfed agriculture and classified as semiarid (Batisani and Yarnal, 2010), is selected as a study area. Studies conducted by Parida and Moalafhi (2008), indicate that rainfall has decreased across Botswana since 1979/80. A study by Batisani (2012) revealed significant correlations between rainfall variability and cereal yields. The study however did not incorporate the influence of ENSO and temperature on crop yields. Further still, the study did not provide any insights on future crop production trends. With overwhelming evidence of global warming, temperature may not be ignored in any climate impact study. Hence this study proposes the investigation of the association of crop yields with climate variability expressed through climatic indices such as Aridity index (AI) and Standardised precipitation evapotranspiration index (SPEI) under the influence of ENSO. These two indices incorporate both rainfall and temperature in their computations. Due to the complexity of climate dynamics, this study proposes the use of Artificial Neural Network (ANN) which mimics neural biological signals similar to human reasoning abilities (Byakatonda et al., 2016; Masinde, 2014) to make projections of crop yields. Nonlinear Autoregressive with Exogenous input (NARX) a specialized neural network for time series prediction with feedback connections is proposed for this task. NARX is a class of Dynamic Recurrent Neural Networks (DRNN) which has been proven to perform well mainly due to the time delay and feedback loops that are absent in static neural networks (Gao and Meng Joo, 2005; Guo and Xue, 2014; Lahmiri, 2016; Menezes and Barreto, 2008). In summary, the current study aims at investigating the influence of climate variability in form of climatic indices and length of the rainy season on maize and sorghum yields and at the same time provide crop yield projections for the next 5 years. The study specifically intends to determine the association between crop yields and 1) monthly AI, AI moving averages at 3, 6 and 12 months; 2) SPEI at timescales of 1, 3, 6 and 12 months; 3) southern oscillation index (SOI); 4)length of the rainy season; and 5) provide 5 year projections of maize and sorghum yields.

2. Data and methods

2.1. Data

Data used in this study comprised of locally observed meteorological times series, records of southern oscillation index (SOI) and crop yields. Crop yield data spanned a period from 1978/79 to 2013/14 prompting the use of climatic data covering the same time period.

2.1.1. Climatic data

Meteorological data was provided by the Department of Meteorological Services (DMS) of Botswana from 12 synoptic stations situated in the 5 agricultural zones as shown in Table 1. Total rainfall for the crop growing season (November- May) for the study area ranges from 600 mm in the northeast at Kasane to 250 mm in the southwest at Tsabong as shown on Fig. 1(a). Rainfall is highly variable with coefficients of variability (CVs) ranging from 48% at Tsabong to 27% at Kasane (Fig. 1(b)) bringing more uncertainties to rainfed agriculture, especially in the southwest. Mean seasonal maximum and minimum temperature of 32 °C and 18 °C respectively are experienced across Botswana.

The influence of ENSO on crop yields is studied using SOI which quantifies the magnitude of ENSO based on atmospheric pressure. Strongly negative values of SOI are associated with strong El Niño responsible for droughts in the southern hemisphere (Hoell et al., 2015; Rojas et al., 2014; Zaroug et al., 2014). Strongly positive SOI values, on the other hand, are associated with strong La Niña responsible for negative temperature anomalies that accounts for rain periods in Botswana. Data on SOI was obtained from the National Climate Data Center of National Oceanic and Atmospheric Administration (NOAA-NCDC, 2016). For analysis, the SOI data is arranged at monthly and seasonal scales based on the crop growing season.

2.1.2. Crop yield data

Yields of two main food crops in Botswana viz; maize and sorghum were obtained from the Ministry of Agriculture. The locations from which the data were collected in the respective agricultural zones are shown in Table 1 and Fig. 1(b). These locations are mainly situated in the Limpopo river basin in the east and southeast as well as Okavango basin in the north. The central and western areas of Botswana are predominantly dry bordering the Kalahari Desert hence the sparse distribution of agricultural locations. Crop yield data was aggregated according to agricultural zones as indicated in Table 1. The length of the growing season is deduced from the onset and cessation of rain dates. Rain onset across the study area occurs during November-December period and cedes between April and May. Areas in the north have earlier onset compared to southern drier locations. Both maize and sorghum are rainfed with yields in most cases closely following rainfall

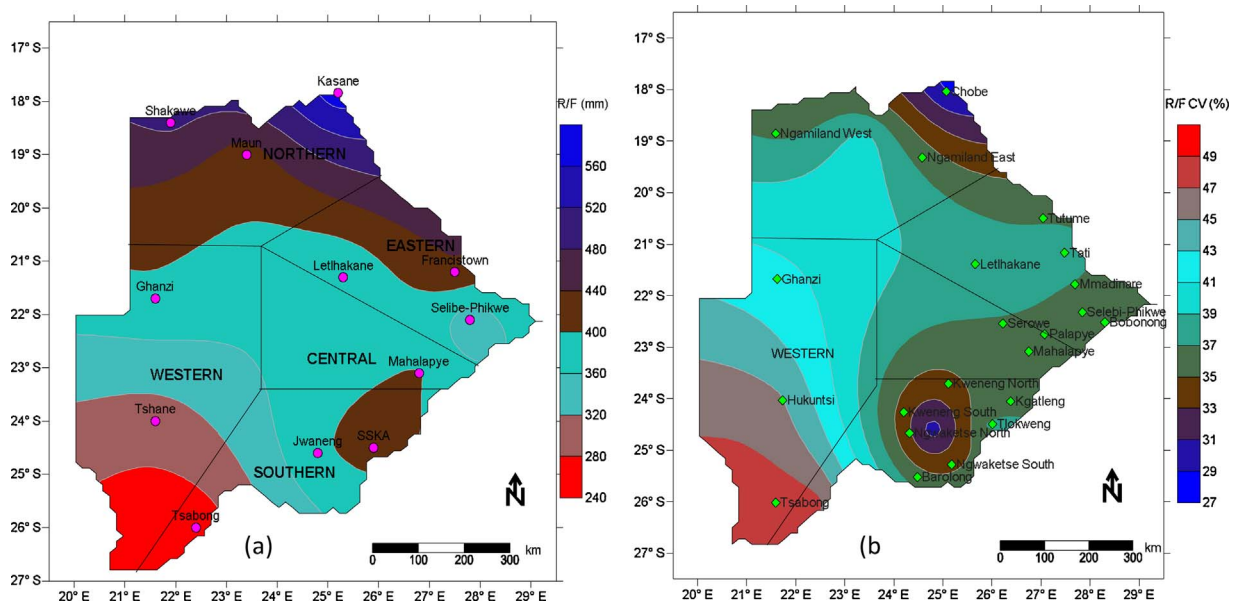

Fig. 1. Seasonal rainfall distribution for the cropping season (November-May) (a) Total rainfall, synoptic stations and agricultural zones (b) Coefficient of variation of seasonal rainfall and crop yield data locations in diffferent regions.

patterns. A case in point is the above normal rainy year of 1995/96 which resulted in sudden increase in yields as shown in Fig. 3. That year was also characterised as a La Nina year by Golden gate Weather Services (2017), indicating a high possibility of ENSO influence on yields over the study area. The mean maize yield varies from 142 kg/ha in the southern region to 43 kg/ha in the western region. Sorghum yields range from 183 kg/ha in the southern region to 19 kg/ha in the western region. Just as the case of rainfall, crop yields experience even higher variability. The western region located in the Kalahari Desert exhibits coefficients of variability (CVs) of 130% while the lowest of 75% in maize yields is experienced in the southern region. Sorghum yields show the highest CV of 130% in northern and central regions, while the lowest CV of 73% was recorded in the southern region.

2.1.2.1. Crop data smoothing. Since the aim of this study is to investigate the influence of climatic factors on crop yields, attempts are made to minimize effects of other technological interventions that could influence yield trends. The technique used in this study is the Holt-Winters double exponential smoothing. This technique is suitable as it takes care of time dependent trend which is inherent in crop yield time series resulting from rainfed agriculture. It in the process assigns exponentially decreasing weights resulting in recent observations having more effect on data smoothing (LaViola, 2003; Lim and McAleer, 2001). The formulation as suggested by Lim and McAleer (2001) and applied in Croakin and Tobias (2006) states that, for a given period t, the smoothed crop yields C_t is obtained from,

$$C_t = \alpha y_t + (1 - \alpha)(C_{t-1} + a_{t-1}) \text{ for} 0 \leq \alpha \leq 1 \quad (1)$$

Where a_t takes care of the trend in the data at time t and is given by;

$$a_t = \beta(C_t - C_{t-1}) + (1 - \beta)a_{t-1} \text{ for } 0 \leq \beta \leq 1 \quad (2)$$

And y_t are observed crop yields at any time t, α and β are smoothing constants obtained via the nonlinear optimization of Levenberg-Marquardt algorithm through the damped least squares as detailed in Lourakis (2005). The initial values of $C_{t=1} = y_1$ and a_1 is given by;

$$a_{1=}\frac{(y_n - y_1)}{(n-1)} \quad (3)$$

Where n is the total number of years under observation.

2.2. Methods

2.2.1. Determination of rain onset and cessation dates and length of the rainy season

The onset criteria is adopted from studies by Araya and Stroosnijder (2011) and Byakatonda et al. (2016), who stated that, onset is assumed to occur on a Julian day where accumulated pentad rainfall exceeds or equals 50% of accumulated potential evapotranspiration over the same time period. This holds provided these conditions are maintained for the next 10 days and total rainfall within this period does not fall below 25 mm. There must also be no dry spell exceeding 10 days within 30 days of assumed onset date. Similarly cessation is assumed to occur on the 7th day after 50% of the pentad accumulated potential evapotranspiration exceeds that of pentad rainfall. For this to occur, 10 days of dry spell should follow the period of deficit. The length of the rainy season is then determined as the number of days between onset and cessation of rain dates.

2.2.2. Determination of drought severity index

The magnitude and duration of drought in this study is expressed in form of standardised precipitation evapotranspiration index (SPEI). SPEI is a multiscalar index that is determined at different timescales allowing quantification of effects of drought on various components of the hydrological cycle including soil moisture and ground water supply responsible for crop growth. In this study, SPEIs are aggregated at timescales of 1 month (SPEI-1) for short term droughts (moisture deficit), 3 months (SPEI-3) for medium term droughts, 6 months (SPEI-6) accounting for seasonal droughts and 12 months (SPEI-12) represents long term droughts. Dry/wet spells at every timescale are determined for each month and the entire growing season. For instance, SPEI-6 for April takes into account accumulated moisture deficit/surplus for April and the previous 5 months. The computational steps of SPEI as applied in Vicente-Serrano et al. (2010), Stagge et al. (2015) and Byakatonda et al. (2016) are as follows;

1. Computation of monthly potential evapotranspiration (ET_0) using the Hargreaves equation. This method is used due to absence of detailed climatological data on relative humidity, wind speed and sunshine hours (Allen et al., 1998; Cai et al., 2007; Stagge et al., 2014).
2. A climatic water balance in form of the difference between monthly

Table 2
Standardised precipitation evapotranspiration index (SPEI) classifications (Yu et al., 2014).

SPEI	SPEI classification
< −2	Extreme Drought
−1.99 to −1.50	Severe Drought
−1.49 to 1.00	Moderate Drought
−1.00 to 1.00	Near Normal
1.00 to 1.49	Moderately Wet
1.50 to 1.99	Severely Wet
> 2.00	Extreme wet

The monthly SPEI values are also averaged for the entire crop growing season to establish an aggregated association at harvest.

rainfall and ET_0 is computed and aggregated at the time scales of 1, 3, 6 and 12 months.

3. An appropriate probability density function (pdf) fitting the water balance series is determined using L-moments and probability weighted moments (PWM). A cumulative density function (CDF) of the pdf is then determined. The generalized logistic distribution was identified to fit the water balance series generated from this study.
4. Through the Gaussian transformation of the CDF, the SPEI values are obtained. Negative values of SPEI signify dry conditions while positive values represent wet conditions classified according to Table 2.

2.2.3. Determination of aridity index (AI)

Aridity index is used in this study to understand the effect of long term moisture deficiency over the study area. It is used to measure the extent of dryness of a given climate and sometimes used in climate classifications (Maliva and Missimer, 2012). The aridity index relates the available rainfall with ET_0. For applications of AI to soil moisture deficit and hence agriculture, the De Mortone formula is used. AI_i for a given year i as defined by De Martonne (1926), applied in Livada and Assimakopoulos (2007) and Zhang et al. (2009) is presented as;

$$AI_i = \frac{12P_i}{10 + T_i} \quad (4)$$

Where P_i is the monthly rainfall for year i and T_i is the monthly mean air temperature. When aridity index falls below 20, the actual evapotranspiration starts to drop below potential evapotranspiration and hence periods of moisture deficit leading to plant water stress. Prolonged periods under deficit conditions may lead to yield loss. Time series of AI are smoothened to minimize fluctuations over different timescales of 3, 6 and 12 months. The original and smoothened series are then used for correlation analysis with detrended crop yields. The different moving average window periods is also used to identify the timescale that closely associates with crop yields.

2.2.4. Association of climatic indices and length of the rainy season and crop yields

The effects of climatic variables on crop yields are investigated through statistical analysis. Due to the complexities in climate dynamics and sometimes nonlinearity in the relationships between crop yields and climate variables coupled with small samples, a non parametric Spearman rank correlation is used in this study to establish monotonic relationships. The strength of the association between crop yields and climatic indices such as AI, SPEI, SOI and LRS is determined through bivariate correlation analysis. A correlation matrix of different pairs is then built to identify significant associations at 95% confidence level. Even where strong associations exist, projections cannot be made based on these relationships due to the complexity of climatic dynamics. For this reason, ANNs are employed to project crop yields using climatic indices as predictors.

2.2.5. Projections of crop yields using artificial neural network (ANN)

Artificial neural networks (ANNs) are a category of nonlinear models that are flexible and can easily discover interrelations between different data inputs. With sufficient number of neurons, ANNs learn from experience to estimate more complex situations with uttermost accuracy. In general, ANNs comprises of three layers viz; input, hidden and output layers. A number of ANN configurations exist for different applications and have been adequately discussed in various literature (Chang et al., 2015, 2014; Masinde, 2014; Mishra and Desai, 2006; Mishra and Singh, 2011; Morid et al., 2007). Among the numerous configurations, the Nonlinear Autoregressive with Exogenous input (NARX) model has been found to provide better performance in time series predictions (Chang et al., 2015; Gao and Meng Joo, 2005; Menezes and Barreto, 2008; Ranjit and Sinha, 2016). Equally the NARX model comprises of input, hidden and output layers but with time delay and feedback connection from the output to the input layer to enable the model operate in both open loop for a one step ahead prediction and

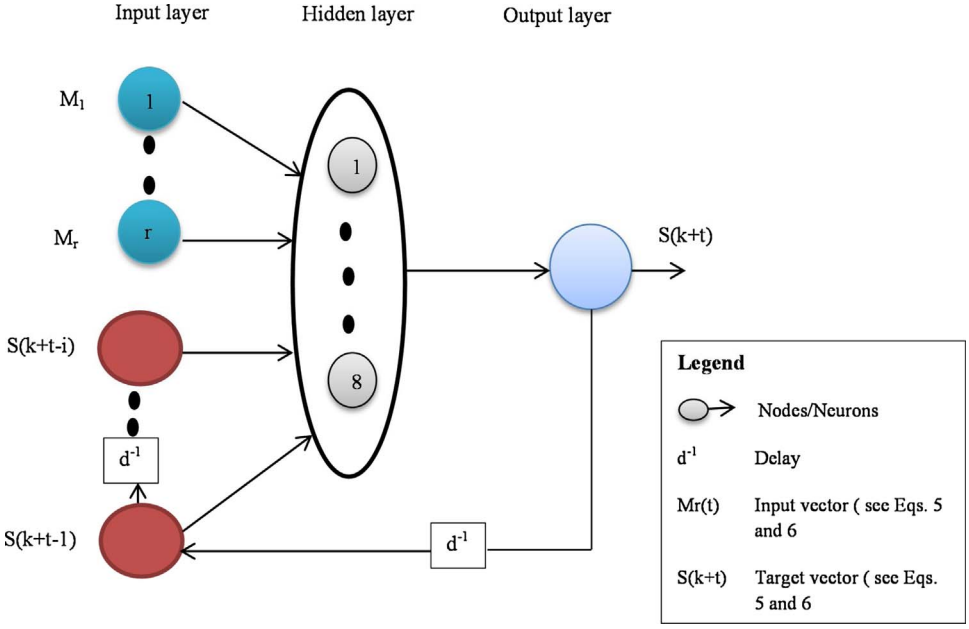

Fig. 2. Nonlinear autoregressive with exogenous input (NARX) model architecture showing the input, hidden and output layers and their flow directions.

closed loop for multistep ahead predictions as shown in Fig. 2. The NARX model building process is as follows;

1. Data preparation

Data is prepared by identifying the exogenous inputs which are known factors that affect crop yields, in this study they are obtained from the correlation matrix in section 2.2.4. The model inputs are standardised precipitation evapotranspiration index, aridity index, southern oscillation index and length of the rainy season. Crop yields are the target series and at the same time an autoregressive component of the model.

2. Hidden layer and number of neurons

Selection of the number of hidden layers and neurons in this layer is made based on various combinations. In this study, one hidden layer with 8 neurons was found sufficient to learn and map well the inputs. The final combination of hidden layers and neurons is selected based on the combination that presents the lowest error between the output and targets.

3. NARX model architecture and training

The NARX model is a multistep ahead prediction ANN model that makes 5 years predictions in this study. The nonlinear model for k steps ahead can be presented mathematically as;

$$\hat{S}(t+k) = f[\hat{S}(t+k-1), ...,\hat{S}(t+k-i); M_r(t)] \quad (5)$$

Where $M_r(t)$ is the input vector with $r = 1,.,4$ and $S(t+k)$ is the output at time step t until k values are generated. For this study $k=5$ while f(.) is a nonlinear mapping function approximated during model training based on the combination that gives the minimum error. During training, the model makes a one step ahead prediction and runs in open loop mode with the mapping function in equation 5 modified to;

$$\hat{S}(t+1) = f[S(t), ...,S(t+1-i); M_r(t)] \quad (6)$$

In the open loop mode, the mapping function uses recorded data of crop yields. The training is done without k most recent values which are used in the validation of the predictions.

4. Crop yield projections

Model projections are done in a closed loop mode where current projections are fed back into the input layer to generate new ones recursively. The most recent k predictors are used to generate these projections with the corresponding target series used for validating them. Performance of the model is evaluated using the mean square error (MSE) during training and prediction phases. Further still, performance is evaluated through regressions between outputs and targets during training, testing and validation. Relationships are established between outputs and targets from which a coefficient of correlation (r) is obtained. The output-target combination that gives the highest r and lowest MSE is selected.

3. Results

The double exponential smoothing technique has demonstrated its ability in detrending crop yield data as shown in Fig. 3. The detrended crop yields of maize and sorghum are those analysed and reported in this section. The bivariate correlation analysis was used to investigate the influence of climatic indices on crop yields from November to May (the growing season). The analysis was done for each month of the growing season to identify the period that may critically affect crop yields. Only results of significant associations between climatic indices and crop yields are reported here .

3.1. Associations between crop yields and aridity index (AI) at 1 month timescale

Results from correlation analysis between maize yield and AI original series are presented in Table 3. These results indicate that, in the southern region, AI accounts highly for variability in maize yield with significant correlations throughout the growing season. The months of December and January recorded the highest correlations of 0.78 and 0.77 respectively. This period also coincides with kernel and pollen shed development for maize grown in the study area. A correlation of 0.73 was also recorded for the entire growing season in this region. In the central region, only months of December and May showed significant correlations. This implies that yields are likely to be affected if moisture deficit is recorded at kernel development and grain filling stages during the maize growth cycle. Similarly in the eastern region, only January and May together with the growing season had significant correlations. The highest correlation in this region was 0.47 registered for the entire growing season. The northern region recorded a significant correlation of 0.41 in February. Months of January, March, April and May together with growing season correlations showed significant associations for the western region. The highest correlation of 0.47 was recorded for the entire growing season in this region.

From the correlations between AI original series and sorghum yield (Table 3), each month of the growing season recorded significant correlations in the southern region. December recorded the strongest correlation of 0.79 while for the entire season it was 0.64. AI accounted for at least 60% in sorghum yields variation in all the months of the growing season in the southern region. AI accounted for the highest variation of 50% in sorghum yield in the month of May for the central region. The rest of the cropping season recorded no significant correlations in this region. The eastern region had significant correlations in December, January and for the entire growing season which recorded the highest correlation of 0.52. Northern region registered a highest correlation of 0.62 in December with 0.34 recorded for the growing season. The western locations registered their strongest association of 0.48 in March and a crop season's correlation of 0.43.

3.2. Associations between crop yields and aridity index (AI) at moving averages of 3, 6 and 12 months timescale

Results of correlation analysis between AI at 3 months moving average and maize yield are presented in Table 4. They do not show much departure from the results of correlations with AI original series presented in Table 3. The strongest association of 0.75 was recorded in January for the southern region. During kernel, pollen shed and silk formation period for the maize crop i.e. January, February and March, AI was found to account for more than 70% of the variations in maize yield in the southern region. At the same time, a significant correlation of 0.74 was registered for the entire growing season. Similarly, all the months of the growing season recorded significant correlations in the southern region. However the central region only registered a significant correlation of 0.36 during January. The eastern region registered significant correlations in January and for the entire growing season of 0.37 and 0.38 respectively. There were no significant correlations observed in the northern region at this timescale. However in the western region, significant correlations were registered in January, February, March, May and for the entire season with the highest correlation of 0.38 registered in January. This implies significant correlations were registered during kernel development, flowering through to full kernel capacity and full maturity.

The 3 months AI moving average correlations with sorghum yield are presented in Table 4. From these results, the southern region still showed significant correlations for the entire growing season. The strongest association of 0.70 was recorded in January while the entire growing season registered 0.64 in this region. In the central region, a significant correlation of 0.35 was observed in February a period of half bloom for the sorghum crop across the study area. Significant correlations at 3 months moving average were only observed in January and for the entire crop season of 0.35 and 0.40 respectively in the eastern region. The northern region experienced the strongest association of 0.56 in January. A correlation of 0.33 was also registered for the entire growing season. The western region recorded significant correlations

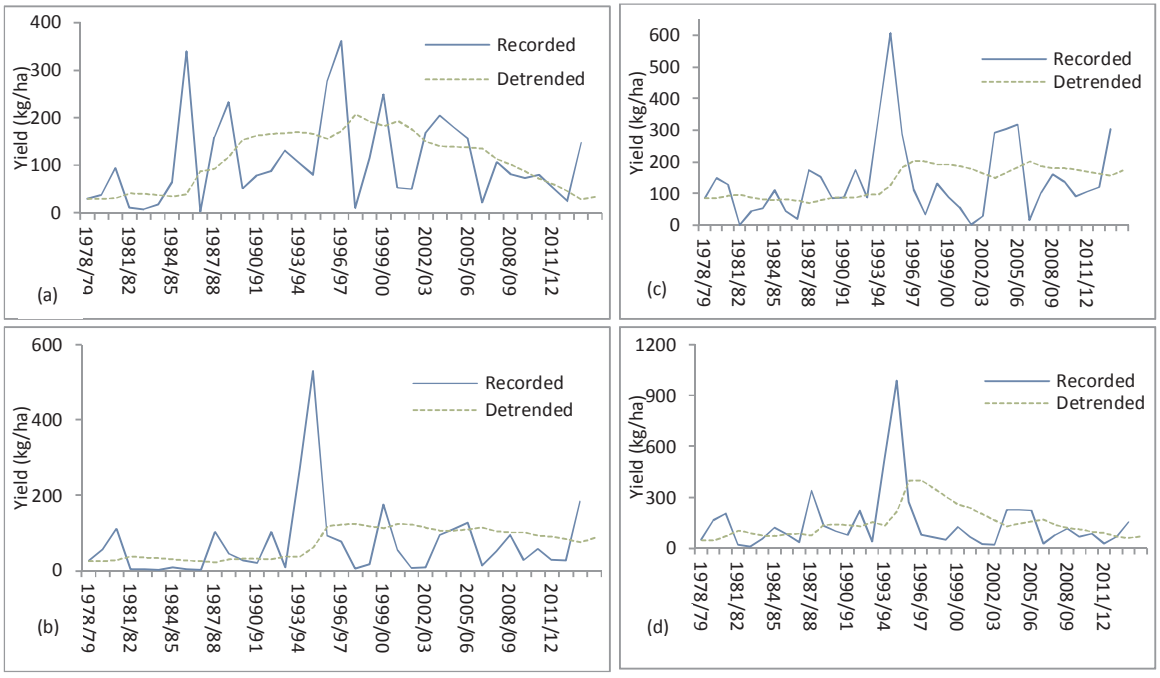

Fig. 3. Maize and sorghum yields (recorded and detrended) in selected regions (a) maize-Northern, (b) Maize-Central, (c) Sorghum-Eastern, (d) Sorghum-Central.

during months of February, March and May, a period of pinnacle development, flowering and grain filling. The strongest correlation of 0.40 was recorded for both March and May towards full maturity of sorghum in this region.

Results from analysis of 6 months AI moving average correlations with maize yield are also presented in Table 4. From these results, the southern region recorded significant correlations throughout the growing season just as is the case at lower time scales. The highest correlation of 0.77 was registered in May. The central region correlations were mainly weak with none of them being significant. The eastern region equally recorded weak correlations with significant values only observed in April and for the cropping season of 0.34 and 0.37 respectively. The northern region experienced significant correlations in November, December, January, April and for the entire growing season. The strongest association of 0.43 was registered in November at tillering stage. The western region also had significant correlations during the months of February, March, April, May and the entire growing season.

At 6 months AI moving average correlations with sorghum yield (Table 4), the southern region indicated significant correlations for the whole season with AI accounting for more than 60% in sorghum yield variation. The strongest association of 0.68 was registered in May together with a correlation of 0.64 for the entire growing season. However the central region only registered a significant correlation of 0.34 in February. The eastern locations showed no significant correlations during the period of study. In contrast, the northern region registered significant correlation of 0.36 in March, 0.37 for both April and May. The western region had only April and May with significant correlations of 0.35 and 0.44 respectively.

Results from the 12 months AI moving average correlations with maize yield (Table 4) indicate that up to 70% in yield variation is accounted for by AI during the months of November, December, January, May and for the entire growing season in the southern region. The strongest association of 0.72 was recorded during the months of December and May for this region. None of the months registered a significant correlation in the central region. In contrast, the eastern and western regions registered significant correlations throughout the growing season. The strongest correlations in these regions were 0.50 and 0.42 for eastern and western regions respectively, recorded in December. Equally the northern region registered significant correlations throughout the growing season except in the month of November.

At 12 months AI moving average correlations with sorghum yield (Table 4), the southern region showed similar patterns to the ones for the lower timescale moving averages. AI still accounted for more than 60% in sorghum yield variations in the southern region. The central and northern regions did not show any significant correlation during the growing season. However, the eastern region exhibited significant correlations of 0.45 and 0.35 in December and January respectively. Similarly the western region showed significant correlations during the months of December and March.

3.3. Associations between crop yields and SPEI at 1 month timescale

Results of the analysis at 1 month SPEI (SPEI-1) with maize yield in Table 3 revealed that, the strongest association between SPEI-1 and maize yield in the southern region is 0.76. This association was registered for both December and January, a period of kernel and brace roots development for the maize crop in Botswana. SPEI-1 accounts for more than 60% of yield variation in the southern region. The entire growing season recorded a correlation of 0.72 in this region. In the central region, correlations were generally weak with highest of 0.46 and 0.34 only observed in May and for the growing season respectively. The eastern region exhibited significant correlations of 0.44 and 0.38 in January and for the entire growing season respectively. The northern region recorded significant correlations in January, February, March and April with the highest correlation of 0.47 realised in February. The western region had significant correlations throughout the growing season with only November and February showing non significant correlations. The strongest association of 0.50 was recorded in January for this region.

Results of correlation between sorghum yield and SPEI-1 (Table 3) presents the southern region with the strongest correlation of 0.78 recorded in December and crop season's association of 0.65. Significant correlations were again observed throughout the growing season. Conversely, for the central region only correlations in May and for the entire season were significant amounting to 0.46 and 0.43 respectively. In the eastern region, significant correlations were observed in December, January, March and for the entire season. The strongest degree

Table 3
Maize and sorghum yield correlations (r) with climatic indices at 1 month timescale.

Location	Climatic indices	1 Month timescale-Maize							
		Nov	Dec	Jan	Feb	Mar	Apr	May	Crop Season
Southern	AI-1	*0.68	*0.78	*0.77	*0.65	*0.66	*0.69	*0.66	*0.73
	SPEI-1	*0.65	*0.76	*0.76	*0.62	*0.65	*0.70	*0.67	*0.72
	SOI	*0.86	*0.82	*0.82	*0.80	*0.80	*0.83	*0.73	*0.85
	LRS								*0.50
Central	AI-1	0.20	*0.34	0.25	0.07	0.02	0.09	*0.56	0.32
	SPEI-1	0.14	0.32	0.24	0.10	0.05	0.13	*0.46	*0.34
	SOI	0.25	0.21	0.24	0.31	*0.35	0.16	−0.12	0.24
	LRS								0.16
Eastern	AI-1	0.06	0.13	*0.46	−0.01	0.11	0.21	*0.34	*0.47
	SPEI-1	0.00	0.19	*0.44	0.04	0.15	0.21	0.06	*0.38
	SOI	*0.37	0.31	0.32	0.30	0.28	*0.34	0.05	*0.38
	LRS								0.05
Northern	AI-1	0.30	0.04	0.32	*0.41	0.30	0.24	0.28	0.21
	SPEI-1	0.23	0.21	*0.34	*0.47	*0.33	*0.33	0.31	0.25
	SOI	0.25	0.30	0.29	*0.37	0.27	0.18	0.20	0.24
	LRS								0.22
Western	AI-1	0.25	0.32	*0.45	0.18	*0.44	*0.37	*0.42	*0.47
	SPEI-1	0.26	*0.35	*0.50	0.19	*0.47	*0.35	*0.40	*0.47
	SOI	*0.39	*0.40	*0.39	*0.39	*0.47	*0.43	0.09	*0.38
	LRS								*0.58
1 month timescale-sorghum									
Southern	AI-1	*0.60	*0.79	*0.69	*0.60	*0.66	*0.63	*0.76	*0.64
	SPEI-1	*0.58	*0.78	*0.67	*0.58	*0.64	*0.61	*0.73	*0.65
	SOI	*0.80	*0.72	*0.74	*0.75	*0.77	*0.72	*0.70	*0.78
	LRS								*0.62
Central	AI-1	0.14	0.27	0.22	0.27	0.21	0.11	*0.50	*0.40
	SPEI-1	0.12	0.28	0.24	0.32	0.23	0.16	*0.46	*0.43
	SOI	0.07	0.08	0.14	0.15	0.17	0.02	−0.15	0.05
	LRS								0.02
Eastern	AI-1	0.22	*0.35	*0.36	0.11	0.30	−0.17	0.30	*0.52
	SPEI-1	0.18	*0.33	*0.38	0.14	*0.33	−0.10	0.08	*0.45
	SOI	0.19	0.21	0.26	0.24	0.31	0.17	−0.19	0.24
	LRS								0.28
Northern	AI-1	*0.54	*0.62	*0.52	0.28	0.26	0.29	*0.33	*0.34
	SPEI-1	*0.56	*0.58	*0.62	0.27	*0.45	0.26	0.26	*0.50
	SOI	*0.42	*0.44	*0.46	0.30	*0.38	*0.43	*0.48	*0.42
	LRS								*0.54
Western	AI-1	0.15	0.28	*0.40	0.18	*0.48	0.29	*0.35	*0.43
	SPEI-1	0.17	0.32	*0.45	0.18	*0.51	0.30	0.32	*0.41
	SOI	0.32	*0.36	*0.33	*0.37	*0.36	0.31	0.02	0.30
	LRS								*0.60

*Significant at 95% confidence interval and LRS = length of the rainy season.

of association in this region was 0.45 registered for the entire growing season. In the northern region, the strongest association of 0.62 was registered in January and the crop season's correlation of 0.50 was also realised. In the western region, significant correlations were observed in January, March and for the entire growing season of 0.45, 0.51 and 0.41 respectively.

3.4. Associations between crop yields and SPEI at 3, 6 and 12 months timescale

Results from analysis of 3 months SPEI (SPEI-3) with maize yield presented in Table 4 show that the southern region still exhibits significant correlations throughout the growing season. These results also reveal that SPEI-3 accounts for more than 60% in maize yield variation in this region. The strongest correlation of 0.74 was recorded in January while the crop season's correlation was 0.70. The only significant correlation in the central region was 0.37 registered in January. Eastern region showed similar patterns as the central region with the only significant correlations of 0.39 and 0.36 registered in January and the entire growing season respectively. In the northern region, a significant correlation of 0.41 was registered for both March and April. The western region showed mostly significant correlations except for November. The strongest correlation of 0.47 was registered in January and February in the western region.

Results from analysis between SPEI-3 and sorghum yield (Table 4) showed the highest correlation in the southern region of 0.67 registered in January. A crop season's correlation of 0.59 was also realised with significant correlations throughout the growing season as the case for SPEI-1. However in the central region, only February showed significant correlation of 0.35. The eastern region registered significant associations in January, March and entire crop season amounting to 0.35, 0.34 and 0.40 respectively. Correlations in the northern region were mainly significant except for the months of November, April and May. The strongest correlation of 0.56 was recorded in January for this region. In the western region, significant correlations were recorded throughout the growing season except at the beginning of the season in November and December. The highest correlation of 0.46 was recorded in March for the western region.

Results from 6 months SPEI (SPEI-6) with maize yield are shown in Table 4. The strongest correlation of 0.95 was recorded in May for the southern region. Significant correlations are recorded throughout the growing season with crop season's correlation of 0.73. The central region showed weak correlations throughout the season while the eastern region registered the only significant correlation in April of 0.35. The northern region generally shows weak correlations for all the months with none of them being significant. The western region mostly

Table 4
Maize and sorghum yield correlations (r) with climatic indices at timescales of 3, 6 and 12 months .

Location	Climatic indices	3 Months timescale-Maize							
		Nov	Dec	Jan	Feb	Mar	Apr	May	Crop season
Southern	AI-3	*0.62	*0.67	*0.75	*0.72	*0.71	*0.65	*0.65	*0.74
	SPEI-3	*0.57	*0.64	*0.74	*0.72	*0.68	*0.67	*0.68	*0.70
Central	AI-3	−0.04	0.28	*0.36	0.24	0.13	0.07	0.10	0.22
	SPEI-3	−0.10	0.23	*0.37	0.25	0.15	0.09	0.13	0.22
Eastern	AI-3	−0.10	−0.01	*0.37	0.30	0.26	0.13	0.21	*0.38
	SPEI-3	−0.20	−0.05	*0.39	0.29	0.27	0.15	0.19	*0.36
Northern	AI-3	0.30	0.15	0.20	0.23	0.31	0.27	0.26	0.23
	SPEI-3	0.22	0.02	0.21	0.32	*0.41	*0.41	0.32	0.20
Western	AI-3	0.17	0.31	*0.38	*0.37	*0.40	0.30	*0.41	*0.36
	SPEI-3	0.18	*0.34	*0.47	*0.47	*0.45	*0.38	*0.43	*0.40
6 Months timescale-Maize									
Southern	AI-6	*0.64	*0.64	*0.69	*0.68	*0.69	*0.75	*0.77	*0.73
	SPEI-6	*0.58	*0.60	*0.67	*0.64	*0.66	*0.69	*0.95	*0.73
Central	AI-6	−0.08	0.19	0.20	0.26	0.21	0.25	0.19	0.20
	SPEI-6	−0.13	0.14	0.26	0.26	0.20	0.23	0.19	0.21
Eastern	AI-6	−0.03	0.01	0.30	0.24	0.25	*0.34	0.32	*0.37
	SPEI-6	−0.19	−0.06	0.23	0.21	0.23	*0.35	0.31	0.25
Northern	AI-6	*0.43	*0.38	*0.35	0.28	0.26	*0.33	0.31	*0.33
	SPEI-6	0.23	0.06	0.20	0.27	0.23	0.22	0.26	0.15
Western	AI-6	0.17	0.18	0.30	*0.35	*0.34	*0.35	*0.41	*0.36
	SPEI-6	0.13	0.19	*0.40	*0.41	*0.45	*0.43	*0.47	*0.39
12 Months timescale −Maize									
Southern	AI-12	*0.71	*0.72	*0.69	*0.68	*0.68	*0.68	*0.72	*0.70
	SPEI-12	*0.70	*0.71	*0.69	*0.66	*0.69	*0.68	*0.67	*0.70
Central	AI-12	0.16	0.23	0.21	0.24	0.20	0.21	0.22	0.21
	SPEI-12	0.14	0.22	0.24	0.23	0.18	0.22	0.21	0.21
Eastern	AI-12	*0.33	*0.50	*0.46	*0.33	*0.33	*0.40	*0.40	*0.40
	SPEI-12	0.32	*0.42	*0.44	0.29	0.27	*0.33	0.32	*0.37
Northern	AI-12	0.32	*0.33	*0.41	*0.43	*0.43	*0.40	*0.43	*0.40
	SPEI-12	0.27	0.28	0.26	0.24	0.28	0.26	0.26	0.26
Western	AI-12	*0.37	*0.42	*0.34	0.31	*0.39	*0.36	*0.39	*0.37
	SPEI-12	*0.40	*0.46	*0.40	*0.38	*0.42	*0.41	*0.44	*0.39
3 Months timescale-Sorghum									
Southern	AI-3	*0.58	*0.66	*0.70	*0.65	*0.66	*0.61	*0.67	*0.64
	SPEI-3	*0.57	*0.63	*0.67	*0.60	*0.63	*0.58	*0.64	*0.59
Central	AI-3	−0.16	0.16	0.27	*0.35	0.27	0.20	0.15	0.26
	SPEI-3	−0.13	0.15	0.31	*0.35	0.30	0.25	0.21	0.28
Eastern	AI-3	−0.05	0.14	*0.33	0.25	0.29	0.13	0.17	*0.38
	SPEI-3	−0.14	0.09	*0.35	0.25	*0.34	0.17	0.19	*0.40
Northern	AI-3	0.24	*0.44	*0.56	*0.49	*0.35	0.25	0.26	*0.33
	SPEI-3	0.24	*0.44	*0.56	*0.49	*0.36	0.25	0.26	*0.33
Western	AI-3	0.08	0.21	0.31	*0.35	*0.40	0.32	*0.40	*0.33
	SPEI-3	0.14	0.30	*0.41	*0.41	*0.46	*0.39	*0.42	*0.38
6 Months timescale-Sorghum									
Southern	AI-6	*0.58	*0.64	*0.65	*0.63	*0.63	*0.66	*0.68	*0.64
	SPEI-6	*0.57	*0.64	*0.64	*0.60	*0.60	*0.59	*0.74	*0.60
Central	AI-6	−0.23	0.09	0.17	*0.34	0.31	0.28	0.29	0.24
	SPEI-6	−0.16	0.11	0.28	*0.36	0.32	0.31	0.30	0.28
Eastern	AI-6	0.00	0.17	0.17	0.13	0.22	0.28	0.27	0.28
	SPEI-6	−0.15	0.09	0.16	0.15	0.25	0.31	0.31	0.25
Northern	AI-6	0.13	0.20	0.29	0.32	*0.36	*0.37	*0.37	0.24
	SPEI-6	*0.40	*0.61	*0.70	*0.59	*0.58	*0.56	*0.48	*0.64
Western	AI-6	0.08	0.10	0.20	0.28	0.32	*0.35	*0.44	0.30
	SPEI-6	0.13	0.18	0.31	*0.38	*0.44	*0.43	*0.50	*0.37
12 Months timescale −Sorghum									
Southern	AI-12	*0.63	*0.63	*0.61	*0.61	*0.62	*0.60	*0.61	*0.61
	SPEI-12	*0.60	*0.61	*0.61	*0.60	*0.61	*0.57	*0.58	*0.61
Central	AI-12	0.19	0.26	0.23	0.31	0.24	0.26	0.27	0.25
	SPEI-12	0.23	0.31	0.30	*0.34	0.26	0.29	0.29	0.31
Eastern	AI-12	0.18	*0.45	*0.35	0.22	0.18	0.23	0.23	0.26
	SPEI-12	0.28	*0.46	*0.35	0.23	0.22	0.27	0.25	0.30
Northern	AI-12	0.17	0.18	0.21	0.19	0.22	0.21	0.20	0.17
	SPEI-12	*0.52	*0.55	*0.63	*0.60	*0.56	*0.55	*0.52	*0.57
Western	AI-12	0.32	*0.38	0.25	0.25	*0.35	0.29	0.32	0.29
	SPEI-12	*0.39	*0.44	*0.37	*0.34	*0.41	*0.38	*0.41	*0.36

*Significant at 95% confidence interval.

registered significant correlations except at the beginning of the cropping season in November and December. The region's strongest correlation was 0.47 realised in May while the entire season it was 0.39.

Results from analysis between SPEI-6 and sorghum yield (Table 4) also showed significant correlations in the southern region for all the months in the growing season. The strongest correlation of 0.74 was observed in May while 0.60 was recorded for the entire growing season. In the central region, only February showed significant correlation of

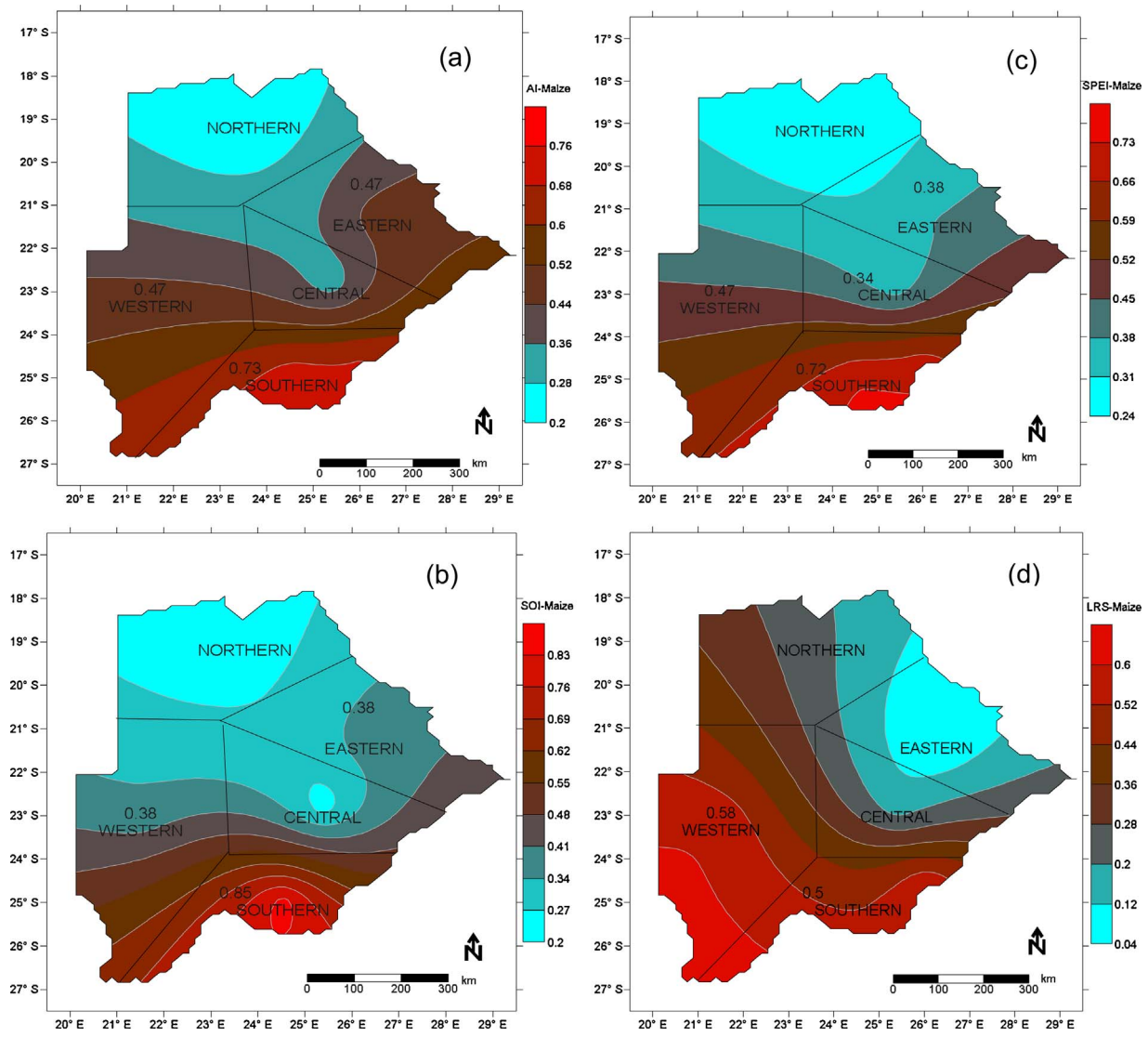

Fig. 4. Spatial distribution of correlations (r) (significant values are shown) between maize yield and (a) Aridity index (AI), (b) Southern oscillation index (SOI), (c) Standardised precipitation evapotranspiration index (SPEI) and (d) Length of the rainy season (LRS).

0.36. In the east, correlations were mainly weak with none of the months showing significant correlations for the entire season. Significant correlations in the northern region were observed for the entire season. The highest variation in sorghum yield that could be accounted for by SPEI-6 was 70% occurring in January in the northern region. The western region showed also significant correlations in February, March, April, May and for the entire growing season.

Results of 12 months SPEI (SPEI-12) with maize yield are also presented in Table 4. These results revealed similar patterns in the southern region as those at lower timescales. The highest correlation of 0.71 in the region was registered in December. A significant crop season's correlation of 0.70 was also realised for the entire growing season. The central region still showed weak correlations with none of them significant. Eastern region showed significant correlations in December, January, April and for the entire growing season. The highest correlation of 0.44 was registered in January in this region. In the northern region non significant correlations were registered for all the months in the growing season. In the western region, all the months including crop season correlations were significant with the highest of 0.46 registered in December.

Results from analysis of correlations between SPEI-12 and sorghum yield (Table 4) indicates that SPEI accounts for 60% in sorghum yield variations for most of the season in the southern region. In contrast, the central region only registered a significant correlation of 0.34 in February. Also in the eastern region, the only significant correlations of 0.46 and 0.35 were registered in December and January respectively. Conversely, the northern region registered significant correlations for the entire season. The strongest correlation in this region of 0.63 was registered in January and 0.57 for the entire growing season. Similarly western region recorded significant correlations for the whole season with the strongest being 0.44 realised in December.

3.5. Association between SOI and crop yields

Results for analysis of the influence of large climatic predictors represented by SOI on maize yield are shown in Table 3. The SOI accounted for the highest variation in maize yield over the study area. The highest correlation of 0.86 was recorded in November in the southern region with crop season's correlation of 0.85 also realised. All correlations were significant for the entire growing season in the southern region. In the central region, the only significant correlation of 0.35 was registered in March while in the eastern region significant correlations were registered in November, April and for the entire growing season. The influence of SOI on maize yield in the northern region was not

statistically significant except for the month of February which realised a correlation of 0.37. In the western region, significant correlations were observed for the entire growing season except May. The strongest association of 0.47 was registered in March with crop season's correlation being 0.38.

Results of correlations between SOI and sorghum yields are also presented in Table 3. These results reveal that in the southern region SOI accounted for up to 80% in sorghum yield variation occurring in November. SOI accounted for 78% of sorghum yield variations for the entire growing season in this region. However in the central and eastern regions, no significant correlations were registered. In the northern region, significant correlations were observed throughout the season except for February. The strongest association in this region was 0.48 registered in May. Significant correlations are further observed in the west for the months of December, January, February and March.

3.6. Association between LRS and crop yields

Results from the investigation of the influence of LRS on maize yield are presented in Table 3. The results are aggregated for the entire growing season. The investigations revealed that, LRS only registered significant correlations in the southern and western regions of 0.50 and 0.58 respectively. For the rest of the study area, maize yield was not significantly associated with LRS.

Associations of LRS with sorghum yield are also presented in Table 3. The LRS accounts for 62% of sorghum yield in the southern region. The central, eastern and northern regions all showed non significant correlations while in the northern region LRS accounted for 54% in sorghum yield variations. In the western region, LRS accounts for 60% of sorghum yield variation.

3.7. Spatial distribution of correlations (r) between crop yields and climatic indices

Spatial representation of the influence of AI and SOI on maize yield in Fig. 4(a) and (b) indicate that yields in the central and northern regions are not significantly influenced by these climatic indices as compared to the south, west and east of the study area. However correlations between AI and sorghum yield (Fig. 5a) were significant in all the regions across the study area. Also the patterns of correlations between maize yield and SPEI-1 Fig. 4(c) reveal similar direction as those of maize yields and AI except that the central region exhibited a significant correlation. Significant correlations which are shown on the maps are mainly observed in the south, east and southeast. Spatial and temporal patterns of AI, SPEI and SOI influence on crop yields indicates a northwest to southeast increasing gradient.

Spatial patterns of correlations between sorghum yields and SPEI-1 in Fig. 5(c) revealed that yields across the study area are significantly associated with SPEI-1. There was no particular gradient observed to describe the pattern of correlations between regions. Presentation of correlations between sorghum yield and SOI at spatial and temporal scales is shown in Fig. 5(b). The distribution show yields in the southern and northern locations being significantly associated with SOI. Sorghum yield in the western, central and eastern regions was not significantly associated with ENSO activities in the Equatorial Pacific. Spatial representations of the influence of LRS on maize and sorghum yields are presented in Figs. 4(d) and 5(d) respectively. Patterns revealed that crop yields in the southern and western regions were significantly affected by variability in LRS which could be attributed to high rainfall variability with CVs greater than 40% in these locations. Yields in the eastern and central regions were not significantly influenced by LRS except the northern locations for sorghum yield. Correlation patterns showed an east to southwest increasing gradient .

3.8. Comparisons between climatic indices and crop yield trends

Plots of detrended yield anomalies and climatic indices such as AI, SPEI, SOI and LRS are presented in Fig. 6. The southern region, where significant correlations have been reported throughout the growing season, is used for illustration purposes. It is evident from the plots that the crop yields followed the spatial and temporal patterns of the climatic indices. From Fig. 6, it was observed that in the year 1995/96 when a yield jump was registered (Fig. 3), a close match between the climatic indices and the yield anomalies was observed. Fig. 6(a) indicates that positive anomalies of aridity index coincided with positive yield anomalies. Likewise in Fig. 6(c) where positive SPEI signifies wet conditions, periods of positive yield anomalies matched with positive SPEI. Similarly positive SOI which is associated with rainy seasons in the study area, are shown in Fig. 6(b) to correspond with positive yield anomalies. Fig. 6(d) also demonstrated how fluctuations in LRS could affect crop yields. The plot shows that the longer the LRS the higher the yield, as demonstrated by the alignment of positive anomalies of LRS and yield.

3.9. ANN performance and projections of crop yields

In this study, performance of the crop yield projection models was evaluated using coefficient of correlation (r) and mean square error (MSE) between model outputs and targets. Results for 5 year projections from the end of the historical period (2013/14) are presented in Table 5 as percentages of the historical period. The MSE results are shown for both open and closed loops. The open loop MSE demonstrated performance during training and one step ahead projections while the closed loop performance evaluated the multistep ahead projections.

For the maize yield projection model presented in Table 5(a), the coefficients of correlation are above 95% at all the locations used in the study. The best performance of 98% was realised in the central and western regions. Plots of the outputs and targets for the maize yield projection model in 3 selected regions are presented in Fig. 7(a)–(c). The plots revealed that the outputs closely fitted the target series, implying the model was in position to learn patterns of the historical inputs and targets to provide projections presented on the same scale. The projections revealed a possibility of a general yield decline from the end of the historical period. The maize yield projections indicate a likelihood of a decline in central and eastern regions for the next 5 years by 51% and 23% respectively. However the north is expected to have yield increase of 52% over the same time period.

Results from the sorghum yield projection model performance are presented in Table 5(b). These results reveal that the coefficients of correlation (r) for this model are greater than 90% with the best performance of 99% registered in the eastern region. Plots of the relationship between outputs and targets are presented in Fig. 7(d), (e) and (f). As the case for maize yield projection model, a close fit between the outputs and targets was observed for the selected regions. In all the selected regions, there is a possibility of sorghum yield decline from the historical period for the next 5 years. The projections revealed that sorghum yield may decline by 70% in the eastern region. Also a yield decrease of 20% is projected for both northern and western regions with marginal changes expected in the central and region.

4. Discussion

4.1. Associations between aridity index and crop yields

Associations between aridity index and maize yield have been analysed at 4 moving average windows as described in section 3.1. The order in magnitude of correlations was observed not to vary substantially with increasing timescale moving average windows. This could be attributed to the fact that during the summer growing season,

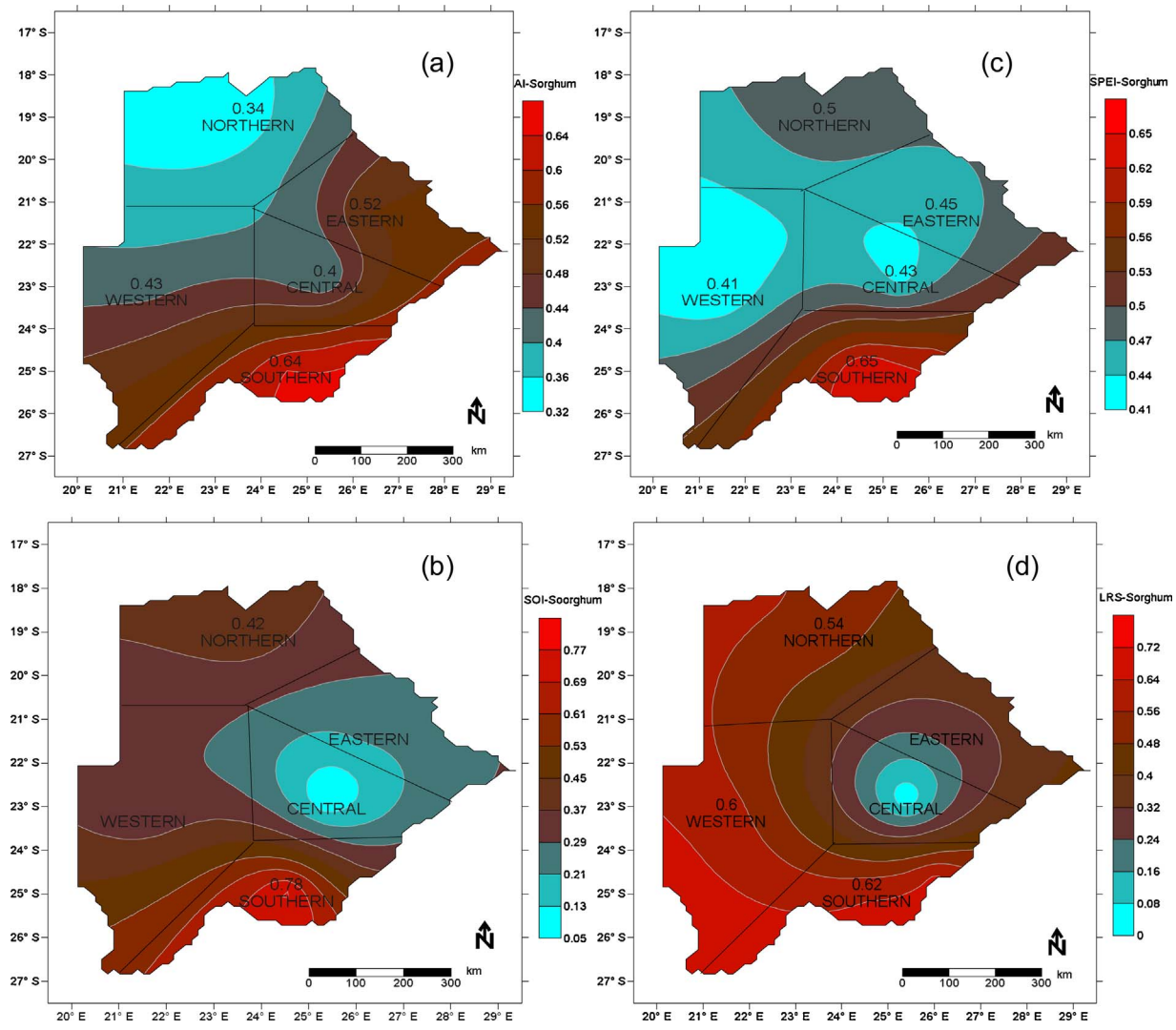

Fig. 5. Spatial distribution of correlations (r) (Significant values are shown) between sorghum yield and (a) Aridity index (AI), (b) Southern oscillation index (SOI), (c) Standardised precipitation evapotranspiration index (SPEI) and (d) Length of the rainy season (LRS).

evapotranspiration (ET) rates are relatively high limiting moisture storage that would be of importance at higher timescales. Evapotranspiration rates have been reported to be 4 times higher than rainfall during summer months (Byakatonda et al., 2016). This revelation implies that monthly aridity index (AI) is sufficient in describing maize yield variability in Botswana. This also corroborates findings by Bannayan et al. (2010) who found zero lags of AI to be sufficient in predicting wheat and barley yields in other semiarid areas of Iran. From the results presented in section 3.1, significant correlations between maize yield and AI were observed throughout the growing season mainly in the southern region. In the central and eastern regions, significant correlations occur mainly during the months of December, January and May. During the period of December-January, maize crop in Botswana undergoes silk formation, kernel and pollen shed development while May is grain filling. During the same period, the sorghum crop undergoes pinacle development and flowering. These are critical phenological stages where plant moisture stress causes yield loss (Darby and Lauer, 2004). This implies that for better yields in the southern and western regions, sustained adequate moisture supply is paramount for the entire growing season. This makes it unfeasible to maintain high yields in these locations. From Fig. 1, these regions are observed to be occupying low rainfall areas with high variability exceeding 40%. Hulme (1992) and Nsubuga et al. (2014) in their studies reported that CVs greater than 30% is an indicator of unreliable rainfall posing high risk to rainfed farming. This may explain the low crop yields in these locations compared to the central, eastern and northern regions. The east and northeastern locations of Botswana with lower CVs are home to most commercial farms for domestic food supply.

As is the case with maize yield, correlations between sorghum yield and AI were performed at 4 moving average windows. The patterns of correlations across regions were similar to those of maize yield and AI with the southern region showing mostly significant correlations. Crop season's correlations of sorghum yields returned weaker associations as compared to those of maize yield at all the 4 moving average windows. This is in agreement with the findings of Critchley et al. (1991) who in their studies established that sorghum's crop water requirement is 500 mm/season compared to 600 mm/season for maize. Further still Gerik et al. (2003) indicates that during tillering and vegetative development stages, sorghum is more tolarant to moisture stress in comparison to maize. This may explain the lower association of sorghum with climatic indices which makes it a better option for the southern locations than maize as a drought resistant crop. Comparing correlations between moving average windows shows no substantial changes in the degree of association. This demonstrates that also monthly AI series can adequately be used to monitor sorghum yield across Botswana.

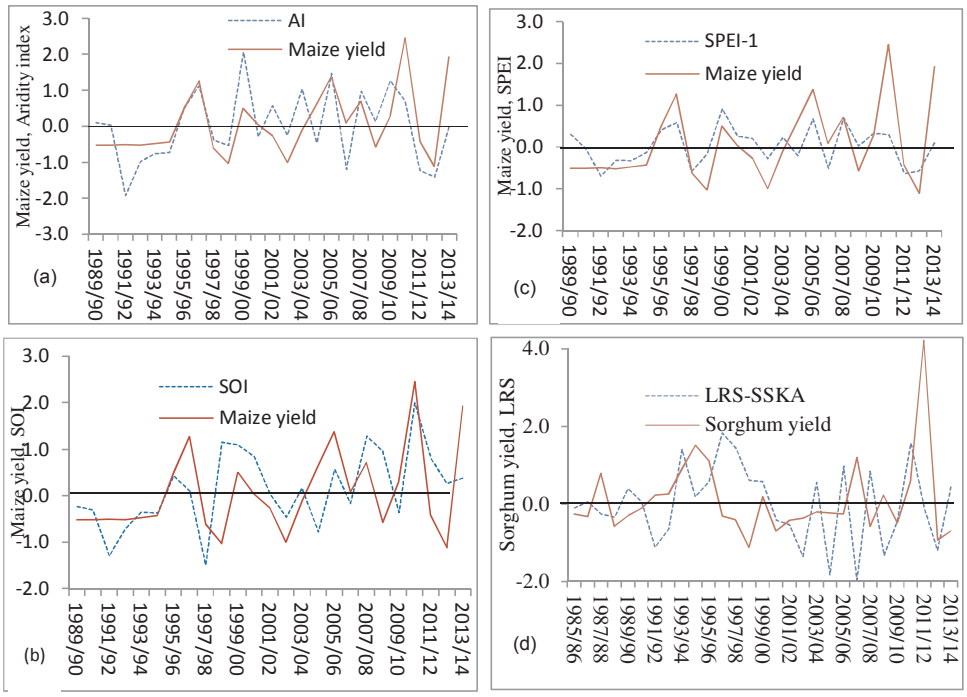

Fig. 6. Comparisons between time series of climatic indices and crop yield anomalies (a) Aridity index (AI) and maize yield, (b) Southern oscillation index (SOI) and maize yield (c) Standardised precipitation evapotranspiration index (SPEI) and maize yield, (d) Length of the rainy season (LRS) and sorghum yield.

4.2. Associations between SPEI and crop yields

The influence of SPEI on maize yield in this study was also investigated at 4 timescales described in section 3.1.2. The patterns of correlations between SPEI and maize yield were also similar to those between AI and maize yield. The southern region still showed significant correlations for the entire growing season implying that any negative SPEI experienced during the season could result in maize yield reduction. The central and eastern regions only showed significant correlations in January and May respectively while in the northern and western they were from January to May for SPEI-1, implying that moisture deficits occuring in these months would lead to yield loss. These periods of significant associations are linked to critical crop growth stages in Botswana. This may explain low crop yields across Botswana compared to the continental average.

Since correlation for both AI and SPEI with maize yield are in the same order across the study area, it could imply that both AI and SPEI are important in monitoring and/or predicting maize yield with equal accurancy. This could be attributed to the fact that in the computation of both AI and SPEI, rainfall and temperature are the main variables. Association of SPI and maize yield have previously been conducted in Botswana by Batisani (2012). In that study, it was found out that there is a significant relationships in the south pointing to the fact that rainfall, rather than temperature, may be the most influencing factor on yield since rainfall is the only variable in SPI.

Similarly, correlations between SPEI and sorghum yield were investigated at 4 timescales. Significant correlations were observed across the study area for the entire growing season. This could be attributed to significant associations registered at critical phenological stages that occured in December, January and May. Further still, SPEI is an aggregation of temperature and rainfall which are known climatic factors that affect crop yields. These factors (temperature and rainfall) have been identified to be influenced by events of global warming (Costa and Soares, 2009; Hänsel et al., 2016). Studies by Rowhani et al. (2011) in Tanzania revealed that variations in rainfall and temperature are injurious to yields of maize and sorghum. From correlations between sorghum yield and SPEI, this study revealed minor variations in correlations at different timescales. This makes SPEI-1 adequate in monitoring sorghum yield across the study area. Since SPEI is a measure of drought severity of a given location, its close association with crop yields, goes a long way in describing how drought is impacting on the food security situation of that location. From drought monitoring strategies, projections of sorghum yield can be made to aid planning.

Table 5
Artificial Neural Network (ANN) model performance and crop yield projections.

Location	Performance based on targets and model outputs			Recorded yield (kg/ha)	Yield predictions as percentage of historical period					
	r	Open loop (MSE)	Closed loop (MSE)	2013/14	Year 1	Year 2	Year 3	Year 4	Year 5	Yield change
(a) Maize yield projection ANN mode										
Southern	0.97	0.012	0.150	175.1	96.6	116.6	85.5	114.4	100.3	10.4
Central	0.98	0.032	0.276	101.7	80.9	82.6	100.6	70.8	102.6	−51.2
Eastern	0.97	0.540	0.054	90.34	66.3	114.4	117.5	85.2	101.5	−22.9
Northern	0.96	0.014	0.064	72.8	182.8	92.1	75.7	114.1	104.7	52.2
Western	0.98	0.322	0.006	68.1	60.5	93.9	121.8	125.2	100.6	−12.7
(b) Sorghum yield projection ANN model										
Southern	0.90	0.023	0.672	213.0	101.3	105.2	88.7	100.3	86.6	−17.9
Central	0.91	0.047	0.174	121.2	167.4	83.4	97.8	80.1	96.4	5.4
Eastern	0.99	0.054	0.157	180.5	78.7	99.3	72.5	62.2	85.8	−69.8
Northern	0.95	0.087	0.432	229.9	54.3	95.5	124.5	90.3	137.7	−19.6
Western	0.97	0.065	0.137	31.0	60.0	104.1	109.6	108.5	106.6	−20.9

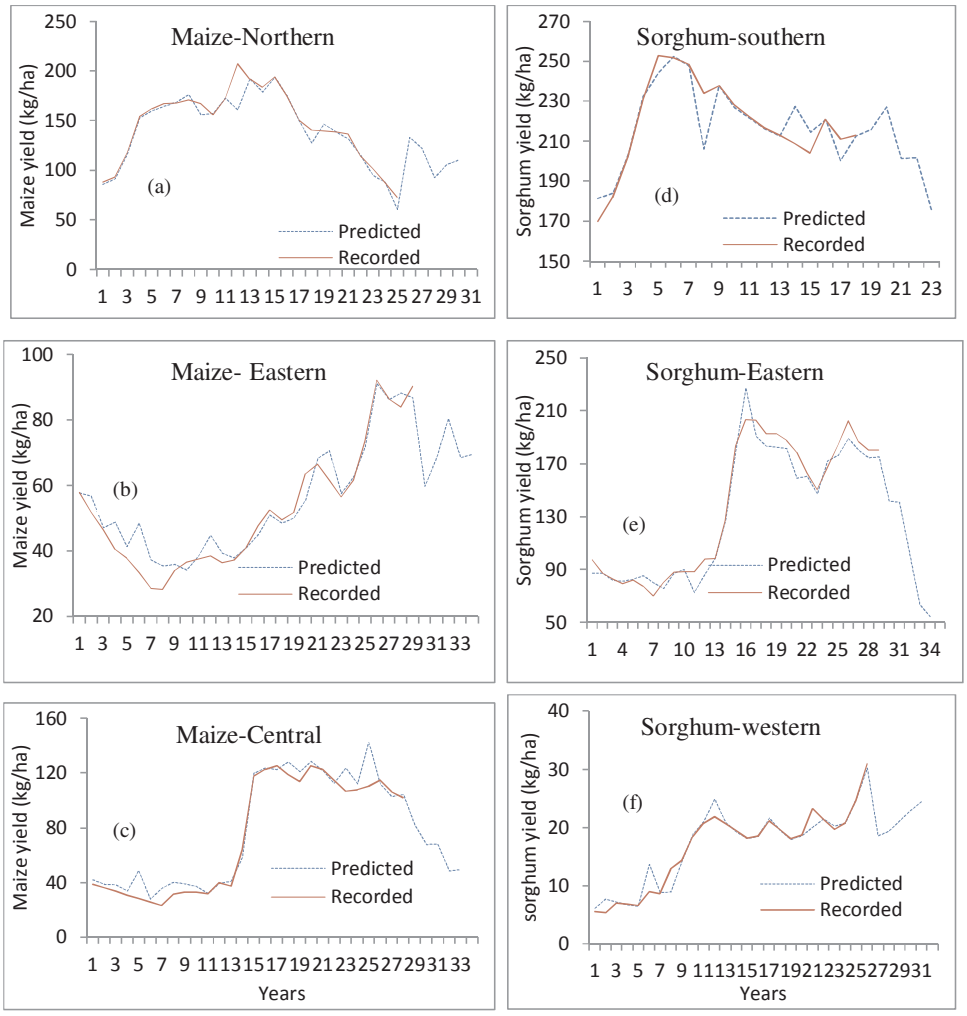

Fig. 7. Artificial Neural Network (ANN) crop yield projection model outputs and targets in selected regions (a) maize yield-northern, (b) maize yield-eastern, (c) maize yield-central, (d) sorghum yield-southern, (e) sorghum yield-eastern and (f) sorghum yield-western.

4.3. Associations between SOI and crop yields

SOI representing large scale climatic predictors has been observed to account for the biggest percentage of maize yield variations in the southern region. This implies that maize yields in regions with significant correlations can benefit from longterm SOI predictions currently ongoing. Based on forecasts of climatic indices such as North Atlantic Oscillation (NOA), Bannayan et al. (2011) demonstrated that barley and wheat yields could accurately be predicted. In Botswana, managers and policy makers in the agricultural sector could use this information to predict yields in these locations at the beginning of the growing season. The rest of the regions with non significant correlations can still benefit from other prediction mechanisms such as ANN used in this study.

Significant correlations between SOI and sorghum yield are also observed over the southern region although lower than those of maize yields. Since it has been indicated that positive SOI are associated with high yields, it means that sorghum is likely to register higher yields than maize under moisture deficit conditions. With high degree of associations between sorghum and SOI, sorghum yield can also benefit from predictions of large scale predictors done by various agencies. However the high association between crop yields and SOI in the region could be injurious to crop production. ENSO has been identified to be closely associated with climate variability in the Equatorial Pacific in teleconnection with the Indian and Atlantic Oceans (Morán-Tejeda et al., 2016; Nicholson et al., 2001). Droughts over southern Africa have also been attributed to ENSO especially during the El Niño phases (Edossa et al., 2014; Usman and Reason, 2004).

4.4. Associations between LRS and crop yields

Results from this analysis reveal a positive association between LRS and maize yield in all regions, however only significant in the southern and western regions. This positive association indicates that the longer the LRS the higher the yields. Amekudzi et al. (2015) in their study found that climate variability has tendency of altering the onset and cessation of rain and hence the LRS. Further still, semiarid areas have been identified to suffer from higher climatic variability than any other region (Byakatonda et al., 2016; Khan et al., 2016; Omoyo et al., 2015). This makes areas in the south and west which are low rainfall areas in Botswana more vulnerable to fluctuations in LRS as a result of increased climate variability and hence low crop yielding areas. This may explain the high associations in these regions.

Correlations between LRS and sorghum yield were significant in the southern and western regions all located in low rainfall areas of Botswana characterised by unreliable rainfall with high CVs. This agrees with studies by Modarres and da Silva (2007) who revealed that drier locations experience higher rainfall uncertainties that affect agricultural production. Yields in regions of central and eastern Botswana were less influenced by fluctuations in LRS and hence registering higher yields compared to southern and western locations.

4.5. ANN performance and projections of crop yields

The multistep ahead NARX model has demonstrated its ability to learn the interelations between associated inputs and target variables as represented by high (r) values and low MSE. This high performance of

NARX in open loop mode gives credence to the yield projections resulting from the trained model. This study is one of its kind where NARX model has demonstrated ability to project crop yields while using ENSO as one of the predictors. Previousely NARX has been used to model water quality and flood heights (Chang et al., 2015, 2014; Menezes and Barreto, 2008). Recent attempts to use NARX for crop yield projections by Guo and Xue (2014) in Australia and Ranjit and Sinha (2016) in India used rainfall and temperature as the main predictors.

Maize yield projections reveal a likelihood of a decline in the central and eastern regions. These regions are among those reported with high yields, this may pose a threat to food security in the near future. However, the northern and southern regions are projected to have yield gains. But the southern locations may not be relied upon to alleviate the food security situation of Botswana since traditionally they are low yield areas (Batisani, 2012).

Sorghum yield projections also revealed possibility of a decline in most locations except the central region which is expected to exprience marginal increases. The highest decline could be experienced in the east followed by the northern region where Botswana derives most of its grain supply under rainfed agriculture. The models reveal that there could be more declines in sorghum yield than maize. Results from these projections could aid planning and adaptive abilities for rural farmers to enable them cope with impacts of climate variability and change.

This study has demonstrated that drier semiarid locations are experiencing high association of crop yields with climate indices and hence likely to be more affected by events of increased incidences of climate variability. Crop yields are already low in these locations implying that conducting business as usual may exacerbate the already fragile environment. Even crop yield projections for the next five years have revealed a general yield decline. This calls for innovations in agricultural practices and technologies to respond to future climate changes. This will require policies and robust institutional arrangements that resonate with these innovations. Policies that are aimed at economic development and poverty alleviation with necessary feedbacks to different levels of stakeholders will go a long way in mitigating impacts of climate change on agriculture. Finally increased resource allocation towards research on cultivars that are tolerant to local climatic conditions is of paramount importance.

5. Conclusions

The influence of climatic indices such as aridity index, standardised precipitation evapotranspiration index, southern oscillation index and length of the rainy season on crop yields of maize and sorghum over semiarid Botswana has been analysed. Investigations were performed through bivariate correlations between the climatic indices and maize yield on one hand and between climatic indices and sorghum yield on the other hand. Two nonlinear with exogeneous input multistep ahead models were also employed to provide 5 year crop yield projections to aid in agricultural planning. From the results and discussions in Sections 3 and 4, the following conclusions are deduced from the study:

1. Maize yields are highly associated with climatic indices in the southern and western regions which are traditionaly low rainfall areas. AI, SPEI, SOI and LRS accounts for a maximum of 73%, 72%, 85% and 50% of maize yield variations for the entire growing season in the southern region respectively. The study also reveals that, the timescale of one month is adequate in monitoring maize yields in Botswana. It is also observed that SOI has the greatest influence on maize yield over other climatic indices further confirming the pronounced effect of ENSO on local climate.
2. Significant associations between sorghum yields and climatic indices are predominant in the southern region. However, they were observed to be lower than those between climatic indices and maize yields. The strongest associations between AI, SPEI, SOI and LRS with sorghum yield for the crop season are 0.64, 0.65, 0.78 and 0.62 respectively. The lower correlations between climatic indices and sorghum yields could mean that sorghum may yield better than maize under climate variability and change.
3. The NARX ANN multistep ahead model has demonstrated ability to make 5 year crop yield projections while using ENSO and climatic indices as predictors. This model could be applied to locations whose climates are known to closely associate with ENSO. The projections reveal a possibility of yield decline over the period of prediction with sorghum declining by 70% over the next 5 years in the eastern region. Maize yields are also expected to decline by 51% in the central region but also the model shows a likelihood of yield gains of 52% in the northern region.

Information generated from this study could contribute towards agricultural planning and management and thus strengthening adaptive capabilities of farmers in order to mitigate impacts of climate variability and change.

Acknowledgements

This study was supported through a scholarship to the first author by the Mobility for Engineering Graduates in Africa (METEGA). Additional support from Carnegie Cooperation of New York through RUFORUM is also acknowledged. Data used was obtained from Department of Meteorological Services and Ministry of Agriculture of Botswana for which the authors are grateful. The authors also appreciate comments from the anonymous reviewer and the editor that enriched the manuscript.

References

Alexandratos, N., Bruinsma, J., others, 2012. World agriculture towards 2030/2050: the 2012 revision.

Allen, R.G., Pereira, L.S., Raes, D., Smith, M., 1998. FAO Irrigation and drainage paper No. 56. Rome Food Agric. Organ. United Nations 56, 97–156.

Amekudzi, L., Yamba, E., Preko, K., Asare, E., Aryee, J., Baidu, M., Codjoe, S., 2015. Variabilities in rainfall onset, cessation and length of rainy season for the various agro-ecological zones of Ghana. Climate 3, 416–434. http://dx.doi.org/10.3390/cli3020416.

Araya, A., Stroosnijder, L., 2011. Assessing drought risk and irrigation need in northern Ethiopia. Agric. For. Meteorol. 151, 425–436. http://dx.doi.org/10.1016/j.agrformet.2010.11.014.

Bannayan, M., Sanjani, S., Alizadeh, A., Lotfabadi, S.S., Mohamadian, A., 2010. Association between climate indices, aridity index, and rainfed crop yield in northeast of Iran. Field Crop. Res. 118, 105–114. http://dx.doi.org/10.1016/j.fcr.2010.04.011.

Bannayan, M., Lotfabadi, S.S., Sanjani, S., Mohamadian, A., Aghaalikhani, M., 2011. Effects of precipitation and temperature on crop production variability in northeast Iran. Int. J. Biometeorol. 55, 387–401. http://dx.doi.org/10.1007/s00484-010-0348-7.

Batisani, N., Yarnal, B., 2010. Rainfall variability and trends in semi-arid Botswana: implications for climate change adaptation policy. Appl. Geogr. 30, 483–489.

Batisani, N., 2012. Climate variability, yield instability and global recession: the multi-stressor to food security in Botswana. Clim. Dev. 4, 129–140.

Byakatonda, J., Parida, B.P., Kenabatho, P.K., Moalafhi, D.B., 2016. Modeling dryness severity using artificial neural network at the Okavango Delta, Botswana. Glob. Nest J. 18, 463–481.

Cabas, J., Weersink, A., Olale, E., 2010. Crop yield response to economic, site and climatic variables. Clim. Change 101, 599–616.

Cai, J., Liu, Y., Lei, T., Pereira, L.S., 2007. Estimating reference evapotranspiration with the FAO Penman–Monteith equation using daily weather forecast messages. Agric. For. Meteorol. 145, 22–35.

Chang, F.-J., Chen, P.-A., Lu, Y.-R., Huang, E., Chang, K.-Y., 2014. Real-time multi-step-ahead water level forecasting by recurrent neural networks for urban flood control. J. Hydrol. 517, 836–846. http://dx.doi.org/10.1016/j.jhydrol.2014.06.013.

Chang, F.-J., Tsai, Y.-H., Chen, P.-A., Coynel, A., Vachaud, G., 2015. Modeling water quality in an urban river using hydrological factors −Data driven approaches. J. Environ. Manage. 151, 87–96. http://dx.doi.org/10.1016/j.jenvman.2014.12.014.

Costa, A.C., Soares, A., 2009. Homogenization of climate data: review and new perspectives using geostatistics. Math. Geosci. 41, 291–305. http://dx.doi.org/10.1007/s11004-008-9203-3.

Critchley, W., Siegert, K., Chapman, C., Finkel, M., 1991. Water Harvesting. A Manual for the Design and Construction of Water Harvesting Schemes for Plant Production. FAO, Rome (Italy).

Croakin, C., Tobias, P., 2006. NIST/SEMATECH e-Handbook of Statistical Methods,

National Institute of Standards and Technology/SEMATECH, (e-book, last updated April 2012): US Commerce Department's Technology Administration.
Darby, H., Lauer, J., 2004. Plant physiology—critical stages in the life of a corn plant [WWW Document]. F. Corn. URL http://corn.agronomy.wisc.edu/Management/pdfs/CriticalStages.pdf. (Accessed 12 June 2017).
De Martonne, E., 1926. A New Climatological Function: The Aridity Index. Gauthier-Villars, Paris, Fr.
Edossa, D.C., Woyessa, Y.E., Welderufael, W.A., 2014. Analysis of droughts in the central region of South Africa and their association with SST anomalies. Int. J. Atmos. Sci. 2014.
Gao, Y., Meng Joo, E., 2005. NARMAX time series model prediction: feedforward and recurrent fuzzy neural network approaches. Fuzzy sets Syst. 150, 331–350.
Gerik, T., Bean, B.W., Vanderlip, R., 2003. Sorghum growth and development. Texas FARMER Collect.
Golden gate Weather Services, 2017. El Niño and La Niña Years and Intensities [WWW Document]. URL http://ggweather.com/enso/oni.htm. (Accessed 20 February 2017).
Guo, W.W., Xue, H., 2014. Crop yield forecasting using artificial neural networks: a comparison between spatial and temporal models. Math. Probl. Eng. 2014. http://dx.doi.org/10.1155/2014/857865.
Hänsel, S., Medeiros, D.M., Matschullat, J., Petta, R.A., de Mendonça Silva, I., 2016. Assessing homogeneity and climate variability of temperature and precipitation series in the capitals of north-eastern Brazil. Front. Earth Sci. 4, 1–21. http://dx.doi.org/10.3389/feart.2016.00029.
Hansen, J., Ruedy, R., Sato, M., Lo, K., 2010. Global surface temperature change. Rev. Geophys. 48.
Hatfield, J.L., Boote, K.J., Kimball, B.A., Ziska, L.H., Izaurralde, R.C., Ort, D., Thomson, A.M., Wolfe, D., 2011. Climate impacts on agriculture: implications for crop production. Agron. J. 103, 351–370.
Helmer, M., Hilhorst, D., 2006. Natural disasters and climate change. Disasters 30, 1–4.
Hoell, A., Funk, C., Magadzire, T., Zinke, J., Husak, G., 2015. El Niño–Southern Oscillation diversity and southern Africa teleconnections during austral summer. Clim. Dyn. 45, 1583–1599.
Hulme, M., 1992. Rainfall changes in Africa: 1931–1960 to 1961–1990. Int. J. Climatol. 12, 685–699.
Khan, M.I., Liu, D., Fu, Q., Dong, S., Liaqat, U.W., Faiz, M.A., Hu, Y., Saddique, Q., 2016. Recent climate trends and drought behavioral assessment based on precipitation and temperature data series in the songhua river basin of China. Water Resour. Manage. 30, 4839–4859. http://dx.doi.org/10.1007/s11269-016-1456-x.
LaViola, J.J., 2003. Double exponential smoothing: an alternative to Kalman filter-based predictive tracking. Proceedings of the Workshop on Virtual Environments. pp. 199–206.
Lahmiri, S., 2016. On simulation performance of feedforward and NARX networks under different numerical training algorithms. Handbook of Research on Computational Simulation and Modeling in Engineering. IGI Global, pp. 171–183.
Li, Y., Ye, W., Wang, M., Yan, X., 2009. Climate change and drought: a risk assessment of crop-yield impacts. Clim. Res. 39, 31–46. http://dx.doi.org/10.3354/cr00797.
Lim, C., McAleer, M., 2001. Forecasting tourist arrivals. Ann. Tour. Res. 28, 965–977.
Livada, I., Assimakopoulos, V.D., 2007. Spatial and temporal analysis of drought in Greece using the Standardized Precipitation Index (SPI). Theor. Appl. Climatol. 89, 143–153.
Lourakis, M.I.A., 2005. A brief description of the Levenberg-Marquardt algorithm implemented by levmar. Found. Res. Technol. 4.
Maliva, R., Missimer, T., 2012. Aridity and drought. Arid Lands Water Evaluation and Management. Springer, pp. 21–39.
Masinde, M., 2014. Artificial neural networks models for predicting effective drought index: factoring effects of rainfall variability. Mitig. Adapt. Strateg. Glob. Chang. 19, 1139–1162. http://dx.doi.org/10.1007/s11027-013-9464-0.
Menezes, J.M.P., Barreto, G.A., 2008. Long-term time series prediction with the NARX network: an empirical evaluation. Neurocomputing 71, 3335–3343. http://dx.doi.org/10.1016/j.neucom.2008.01.030.
Mishra, A.K., Desai, V.R., 2006. Drought forecasting using feed-forward recursive neural network. Ecol. Modell. 198, 127–138. http://dx.doi.org/10.1016/j.ecolmodel.2006.04.017.
Mishra, A.K., Singh, V.P., 2011. Drought modeling–A review. J. Hydrol. 403, 157–175.
Modarres, R., da Silva, V. de P.R., 2007. Rainfall trends in arid and semi-arid regions of Iran. J. Arid Environ. 70, 344–355.
Morán-Tejeda, E., Bazo, J., López-Moreno, J.I., Aguilar, E., Azorín-Molina, C., Sanchez-Lorenzo, A., Martínez, R., Nieto, J.J., Mejía, R., Martín-Hernández, N., Vicente-Serrano, S.M., 2016. Climate trends and variability in Ecuador. Int. J. Climatol. 1966–2011. http://dx.doi.org/10.1002/joc.4597.
Morid, S., Smakhtin, V., Bagherzadeh, K., 2007. Drought forecasting using artificial neural networks and time series of drought indices. Int. J. Climatol. 27, 2103–2111.
Mugalavai, E.M., Kipkorir, E.C., Raes, D., Rao, M.S., 2008. Analysis of rainfall onset, cessation and length of growing season for western Kenya. Agric. For. Meteorol. 148, 1123–1135. http://dx.doi.org/10.1016/j.agrformet.2008.02.013.
NOAA-NCDC, 2016. Southern Oscillation Index (SOI) [WWW Document]. URL www.ncdc.noaa.gov/teleconnections/enso/indicators/soi/data.csv. (Accessed 16 October 2016).
Nicholson, S.E., Leposo, D., Grist, J., 2001. The relationship between El Niño and drought over Botswana. J. Clim. 14, 323–335.
Nsubuga, F.W.N., Botai, O.J., Olwoch, J.M., deW Rautenbach, C.J., Rautenbach, C.J., Bevis, Y., Adetunji, A.O., 2014. The nature of rainfall in the main drainage sub-basins of Uganda. Hydrol. Sci. J. 59, 278–299.
Omoyo, N.N., Wakhungu, J., Oteng'i, S., 2015. Effects of climate variability on maize yield in the arid and semi arid lands of lower eastern Kenya. Agric. Food Secur. 4, 8.
Parida, B.P., Moalafhi, D.B., 2008. Regional rainfall frequency analysis for Botswana using L-Moments and radial basis function network. Phys. Chem. Earth 33, 614–620. http://dx.doi.org/10.1016/j.pce.2008.06.011.
Ranjit, K.P., Sinha, K., 2016. Forecasting crop yield: a compairtve assessment of arimax and narx model 1, 77–85.
Rockström, J., Falkenmark, M., Karlberg, L., Hoff, H., Rost, S., Gerten, D., 2009. Future water availability for global food production: the potential of green water for increasing resilience to global change. Water Resour. Res. 45.
Rojas, O., Li, Y., Cumani, R., 2014. Understanding the Drought Impact of El Niño on the Global Agricultural Areas: An Assessment Using FAO's Agricultural Stress Index (ASI).
Rowhani, P., Lobell, D.B., Linderman, M., Ramankutty, N., 2011. Climate variability and crop production in Tanzania. Agric. For. Meteorol. 151, 449–460. http://dx.doi.org/10.1016/j.agrformet.2010.12.002.
Sivakumar, M.V.K., 2011. Agricultural drought—WMO perspectives. Agricultural Drought Indices Proceedings of an Expert Meeting p. 24.
Some'e, B.S., Ezani, A., Tabari, H., 2013. Spatiotemporal trends of aridity index in arid and semi-arid regions of Iran. Theor. Appl. Climatol. 111, 149–160.
Stagge, J.H., Tallaksen, L.M., Xu, C.Y., Van Lanen, H.A.J., 2014. Standardized precipitation-evapotranspiration index (SPEI): Sensitivity to potential evapotranspiration model and parameters. Proc. FRIEND-Water 367–373.
Stagge, J.H., Tallaksen, L.M., Gudmundsson, L., Van Loon, A.F., Stahl, K., 2015. Candidate distributions for climatological drought indices (SPI and SPEI). Int. J. Climatol. 35, 4027–4040.
Usman, M.T., Reason, C.J.C., 2004. Dry spell frequencies and their variability over southern Africa. Clim. Res. 26, 199–211. http://dx.doi.org/10.3354/cr026199.
Vörösmarty, C.J., Green, P., Salisbury, J., Lammers, R.B., 2000. Global water resources: vulnerability from climate change and population growth. Science (80-.). 289, 284–288.
Vicente-Serrano, S.M., Begueria, S., López-Moreno, J.I., 2010. A multiscalar drought index sensitive to global warming: the standardized precipitation evapotranspiration index. J. Clim. 23, 1696–1718.
Yu, M., Li, Q., Hayes, M.J., Svoboda, M.D., Heim, R.R., 2014. Are droughts becoming more frequent or severe in China based on the standardized precipitation evapotranspiration index: 1951–2010? Int. J. Climatol. 34, 545–558.
Zaroug, M.A.H., Eltahir, E.A.B., Giorgi, F., 2014. Droughts and floods over the upper catchment of the Blue Nile and their connections to the timing of El Niño and La Niña events. Hydrol. Earth Syst. Sci. 18, 1239–1249.
Zhang, Q., Xu, C.-Y., Zhang, Z., 2009. Observed changes of drought/wetness episodes in the Pearl River basin, China, using the standardized precipitation index and aridity index. Theor. Appl. Climatol. 98, 89–99.